JACS
JOURNAL OF THE AMERICAN CHEMICAL SOCIETY
Communication
Cite This: J. Am. Chem. Soc. 2019, 141, 3838−3842
pubs.acs.org/JACS

3d-Metal Induced Magnetic Ordering on U(IV) Atoms as a Route toward U(IV) Magnetic Materials

Vladislav V. Klepov,[†] Kristen A. Pace,[†] Stuart Calder,[‡] Justin B. Felder,[†] and Hans-Conrad zur Loye*[,†]

[†]Department of Chemistry and Biochemistry, University of South Carolina, Columbia, South Carolina 29208, United States
[‡]Neutron Scattering Division, Oak Ridge National Laboratory, Oak Ridge, Tennessee 27831, United States

Supporting Information

ABSTRACT: Uranium(IV) $5f^2$ magnetism is dominated by a transition from a triplet to a singlet ground state at low temperatures. For the first time, we achieved magnetic ordering of U(IV) atoms in a complex fluoride through the incorporation of 3*d* transition metal cations. This new route allowed us to obtain an unprecedented series of U(IV) ferrimagnetic materials of the new composition $Cs_2MU_3F_{16}$ (M = Mn^{2+}, Co^{2+}, and Ni^{2+}), which were comprehensively characterized with respect to their structural and magnetic properties. Magnetic susceptibility measurements revealed ferromagnetic-like phase transitions at temperatures of ∼14.0, 3.5, and 4.8 K for M = Mn^{2+}, Co^{2+}, and Ni^{2+}, respectively. The transition is not observed when the magnetic M cations are replaced by a diamagnetic cation, Zn^{2+}. Neutron diffraction measurements revealed the magnetic moments of 0.91(6)−1.97(3) μ_B on the U atoms, which are only partially compensated by antiparallel moments of 1.53(14)−3.26(5) μ_B on the 3*d* cations. This arrangement promotes suppression of the transition to a diamagnetic ground state characteristic of U(IV), and in doing so, induces magnetic ordering on uranium via 3*d*−5*f* exchange coupling.

Uranium exhibits a wide range of oxidation states, ranging from +2 to +6,[1−3] with the +4 and +6 states being most prevalent in the solid state. The +6 state is exceptionally stable at elevated temperatures in air, making U(VI) compounds among the most studied phases of existing uranium compounds.[4−11] Fully oxidized uranium, however, has an empty 5*f* shell and is thus of little interest for the purpose of studying the magnetic behavior of 5*f* electrons. On the other hand, reduced uranium compounds having 5*f* electron(s) present a valuable opportunity to study their magnetic behavior; complex cases involving exchange coupling with other magnetic elements are of particular interest.[12−19] An understanding of U(IV) compounds magnetic properties has not been fully developed as a result of several challenges posed. The synthetic challenges can be overcome by using the mild hydrothermal synthesis route.[20−27] The most significant challenge present, however, is intrinsic to U(IV), specifically the fact that U(IV) tends to undergo a transition from a magnetic triplet to a nonmagnetic singlet ground state by pairing of the two 5*f* electrons.[28] It has been demonstrated, however, that the crystal electric field effects in some fluoride compounds do not lead to this transition, although the resulting phases, so far, are limited to those that exhibit only paramagnetic behavior.[29,30] In fact, there are only a few binary and ternary U(IV) compounds that have been shown to undergo ferro- or antiferromagnetic transitions, while there is no ferrimagnetic U(IV) compounds reported so far.[31−34]

In order to overcome the singlet ground state transition and to develop an approach to the synthesis of U(IV) magnetic materials, we sought to induce a persistent magnetic ordering on the U(IV) cations by introducing other magnetic ions, such as lanthanides and transition metals (Scheme 1). To achieve this goal, we modified the existing mild hydrothermal synthesis and, by using methanol absorbed by PTFE-liner, employed an additional reducing agent to ensure the U(VI) to U(IV) reduction. This effort has resulted in a novel family of quaternary U(IV) compounds with the composition $Cs_2MU_3F_{16}$, where M is a divalent metal. Magnetic susceptibility measurements on the compounds with the magnetic Mn^{2+}, Co^{2+}, and Ni^{2+} cations exhibit, for complex U(IV) compounds, unprecedented ferrimagnetic phase transitions at low temperatures. The magnetic structures of these compounds, revealed by neutron diffraction, shed light on the origin of this magnetism, highlighting the importance of infinite $(-M-U_3F_{22}-)_\infty$ pillars in its formation. In this Communication, we report on the synthesis, structure, and

Scheme 1. Schematic Illustration of a Successful Route toward Uranium(IV) Ferrimagnetic Materials

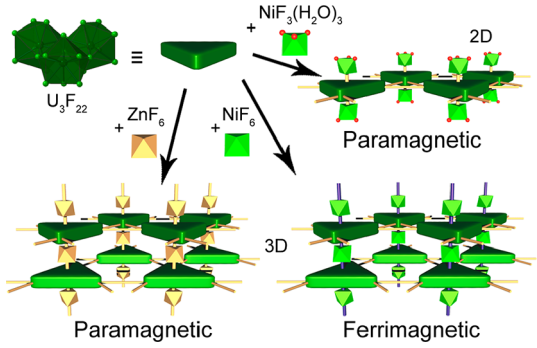

Received: January 10, 2019
Published: February 13, 2019

DOI: 10.1021/jacs.9b00345
J. Am. Chem. Soc. 2019, 141, 3838−3842

fully characterized ferrimagnetic transition in these compounds.

All members of the $Cs_2MU_3F_{16}$ series were obtained via a mild hydrothermal route that involves an in situ reduction step with methanol absorbed by the walls of the reaction vessel. Before each reaction, a 23 mL PTFE liner was charged with 2 mL of methanol and dwelled at 200 °C for 2 h. After methanol was removed from the reaction vessel, uranyl acetate, M^{2+} acetate, and CsCl were loaded into the liner and HF was added as a fluorinating agent. The reaction was carried out at 200 °C for 36 h. The resulting product was washed several times with an excess of deionized water to ensure the dissolution of M fluorides, leaving a phase pure sample of the target phase. Notably, only U(VI) compounds could be obtained if the PTFE liner had not been washed with methanol prior to reaction, suggesting that the methanol absorbed by the liner participates in the U(VI) in situ reduction step along with the acetate anions from the uranyl and M^{2+} salts. We could not reproduce the same effect by adding methanol to the reaction mixture. Single crystals of the compounds with M = Mg^{2+}, Mn^{2+}, Co^{2+}, Ni^{2+}, and Zn^{2+} were obtained in good yield and structurally characterized.

All five compounds crystallize in the centrosymmetric hexagonal $P6_3/mmc$ space group. The main structural feature is a U(IV) fluoride sheet consisting of uranium trimers connected through a μ_3-F^- anion; the trimers connect to each other by edge-sharing. The U(IV) sheets are connected to each other by M^{2+} cations, which creates a channel containing framework in which the Cs atoms are located (Figure 1).

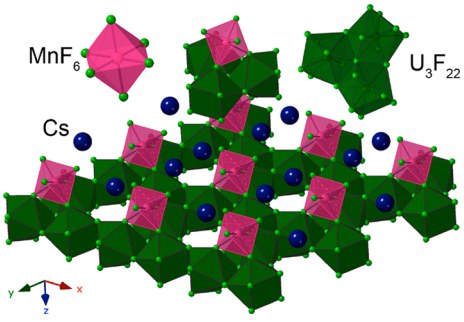

Figure 1. View of the $Cs_2MnU_3F_{16}$ structure. $[U_3F_{16}]^{4-}$ sheets (green) are composed of uranium trimers, which are connected into sheets. The framework is formed by connecting the sheets through MnF_6 (pink) octahedra with cesium atoms (blue) between them.

Three fluoride ions from the top of one trimer and the bottom of another, located above it, are coordinated to the M^{2+} cations. This creates an octahedral coordination environment for M^{2+} consisting of six fluoride ions from two sheets; building unique $(-M-U_3F_{22}-)_\infty$ pillars, which play a crucial role in the magnetism of these compounds.

The molar magnetic susceptibility (χ_{mol}) measurements on the transition metal containing samples were carried out using a Quantum Design Magnetic Properties Measurement System. A Curie–Weiss law fit for $Cs_2ZnU_3F_{16}$ at high temperatures shows a paramagnetic moment of 3.22 μ_B/U(IV) atom. The other three samples, which contain a second magnetic cation, follow the Curie–Weiss law with a transition at low temperatures consisting of a sharp increase in the magnetic susceptibility (Figures 2, S6, and S8). Since the fluoride ion is a weak field ligand, Mn^{2+} in $Cs_2MnU_3F_{16}$ is expected to adopt a high spin configuration with S = 5/2. Co^{2+}, and Ni^{2+} have spins

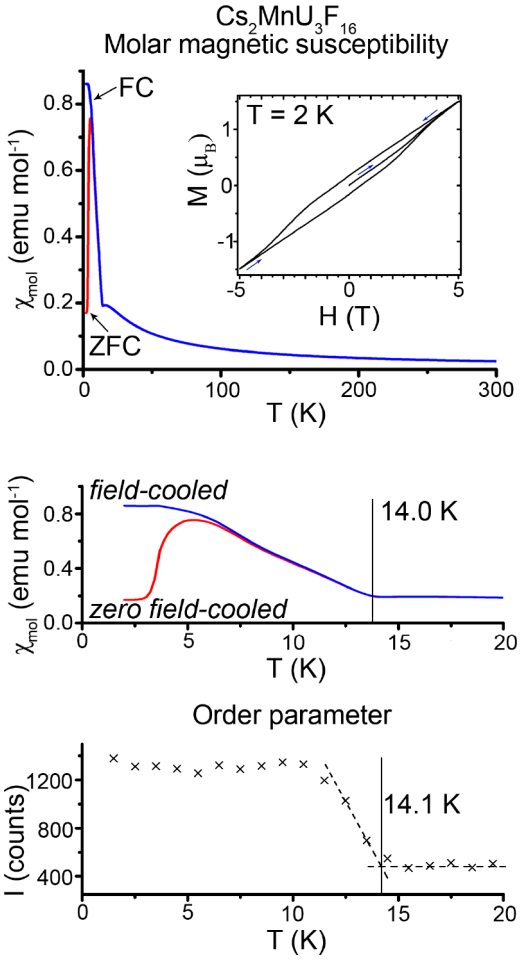

Figure 2. Molar magnetic susceptibility vs temperature (top and middle), magnetization vs field (top, inset), and neutron diffraction intensity of a magnetic reflection at θ = 30.50° vs temperature (bottom) plots for $Cs_2MnU_3F_{16}$.

of 3/2 and 1, respectively. Using the calculated spin-only moments for the M^{2+} atoms and the observed magnetic moments derived from Curie–Weiss law fit at high temperatures, the magnetic moments per U(IV) atom were determined to be (Table S3) 3.22, 3.98, and 3.34 μ_B. Negative Curie–Weiss constants of −41.5, −53.3, and −51.1 K are indicative of antiferromagnetic interactions in the compounds. While the magnetic moments on the U atoms in $Cs_2MnU_3F_{16}$ and $Cs_2NiU_3F_{16}$ agree well with the expected 3.58 μ_B value calculated for the $^3H_4$ ground state of U, $Cs_2CoU_3F_{16}$ exhibits a significant deviation, likely due to incomplete quenching of the orbital contribution to the magnetic moment.

There is a striking difference between the low temperature magnetic susceptibilities observed for the nonmagnetic Zn-containing compound versus the magnetic 3*d* cation containing compounds. $Cs_2ZnU_3F_{16}$ shows a typical transition to a nonmagnetic singlet ground state followed by a drop of the material's magnetization (Figure S6). The Mn-containing compound undergoes an apparent magnetic transition at ∼14.0 K. At 2 K, zero field cooled (ZFC) and field cooled (FC) plots differ significantly, yielding a molar susceptibility of ∼0.17 and ∼0.86 emu mol^{-1}, respectively. The splitting of ZFC and FC curves indicates a ferromagnetic-like ordering in the material. Beginning at ∼7.5 K, both ZFC and FC curves overlap. The magnetization versus field plot (Figure 2, inset)

DOI: 10.1021/jacs.9b00345
J. Am. Chem. Soc. 2019, 141, 3838−3842

collected at 2.0 K shows a hysteresis loop with a coercive field of 0.60 T, supporting the presence of magnetic ordering.

Complete characterization of this intriguing magnetic behavior could only be achieved by determining the magnetic structure, which was accomplished by a series of neutron diffraction experiments performed on the HB-2A diffractometer at the High Flux Isotope Reactor at Oak Ridge National Laboratory (USA).[35,36] Apparent magnetic diffraction peaks are observed in a region of 15−50° at 1.5 K, below the magnetic transitions (Figures S11−S13). For $Cs_2MnU_3F_{16}$, the intensity of the magnetic peak at θ = 30.50° starts to deviate significantly from the background level when crossing the transition temperature at ∼14.1 K, which is in excellent agreement with the value of 14.0 K obtained from the susceptibility measurements. The magnetic reflections were fitted using a k = (1/3, 1/3, 0) propagation vector, leading to a magnetic unit cell that is nine times larger than the nuclear unit cell. The solution to the magnetic structure was found in the $P6_3/mc'm'$ (#193.260[37]) magnetic space group with R_p = 4.67% (Figure 3). In the magnetic structure, the magnetic moments of 1.97(3) and 3.26(5) μ_B aligned parallel to the c axis are found on the U and Mn atoms, respectively.

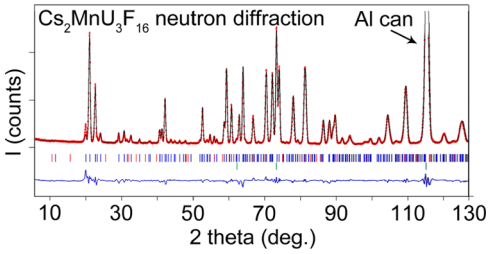

Figure 3. Rietveld refinement plot for the $Cs_2MnU_3F_{16}$.

The magnetic structure of $Cs_2MnU_3F_{16}$ is shown in Figure 4. The manganese atoms and uranium trimers are stacked to form pillars extending along the c axis. In the pillars, the moments on the uranium atoms of the trimer are parallel to each other and antiparallel to the moments on the Mn atoms in the same pillar. Given that the repeating unit of the $(-M-U_3F_{22}-)_\infty$ pillar consists of one Mn atom and one U trimer, there is a net moment of 2.65 μ_B per repeating unit. There are nine pillars in the magnetic unit cell arranged in a hexagonal lattice mode. The net moments on the pillars are aligned collinear with the c axis and tend to be oriented antiferromagnetically with the neighboring pillars, resulting in two magnetically distinct types of pillars. The pillars in the first group have the net moment aligned along the c axis and surrounded exclusively by pillars with the net moment aligned in the opposite direction. The hexagonal arrangement of the pillars and their tendency to align antiferromagnetically results in frustration since the triangular lattice precludes complete antiferromagnetic arrangement of the moments (Figure 4, bottom).[38] Due to this, the second type of pillars cannot be surrounded exclusively by pillars with antiparallel moments, forcing them to have a total of six neighbors, three of which have antiparallel and three of which have parallel moments. The total net moment of the magnetic cell, containing 6 spin up and 3 spin down pillars, is 15.90 μ_B.

The same magnetic structure is observed for the other two analogs, $Cs_2CoU_3F_{16}$ and $Cs_2NiU_3F_{16}$. Smaller moments on the M sites, 1.70(10) and 1.53(14) μ_B correlate with a decrease

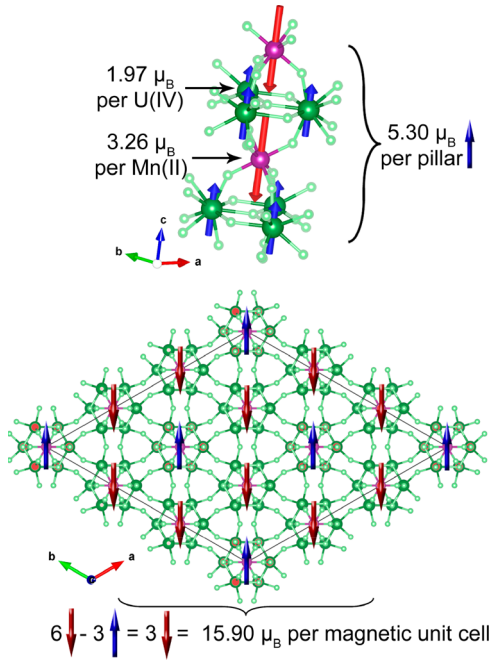

Figure 4. Magnetic structure of $Cs_2MnU_3F_{16}$. Uranium trimers and manganese octahedra carry magnetic moments of 3 × 1.97 and 3.26 μ_B on them. The building units successively combine to form pillars that align along the c axis in a hexagonal mode. Blue and red arrows show magnetic moments aligned parallel and antiparallel along the c axis.

in the moments on the U atoms, 0.91(6) and 0.94(9) μ_B, indicating a dependence of the moments of the U atoms on the moment of the coupled 3d metal cation. The lower moments on the Co^{2+} and Ni^{2+} atoms also result in a decrease in the transition temperatures, which are 3.5 and 4.8 K, respectively.

A comparison of $Cs_2MU_3F_{16}$ and a previously reported $Na_xMU_6F_{30}$ series, which exhibits paramagnetic behavior, can shed light on the structural prerequisites for U(IV) magnetic ordering. The main feature of the $Cs_2MU_3F_{16}$ structure is the presence of infinite $(-M-U_3F_{22}-)_\infty$ pillars and $U_3(\mu_3\text{-}F)F_{21}$ trimers, which are both absent in the other structure type. We performed magnetic susceptibility measurements on $Ni_2(H_2O)_6(U_3F_{16})(H_2O)_3$,[39] which exhibits the same $[U_3F_{16}]^{4-}$ layers found in $Cs_2MU_3F_{16}$ that, however, are separated not by isolated nickel cations, but rather by aquonickel species preventing the formation of $(-M-U_3F_{22}-)_\infty$ pillars and forming $(H_2O)_3Ni-U_3F_{22}-Ni(H_2O)_3$ finite fragments instead. This compound does not undergo a magnetic transition down to 2 K (Figure S18), suggesting that the infinite $(-M-U_3F_{22}-)_\infty$ pillars perform a crucial role in the magnetism of the $Cs_2MU_3F_{16}$ series.

In conclusion, we synthesized a family of unique quaternary uranium(IV) fluorides that exhibit simultaneous spin ordering on U(IV) and M = Mn^{2+}, Co^{2+}, and Ni^{2+} cations at low temperatures. The source of their ferrimagnetic behavior, unprecedented for complex uranium fluoride compounds, is the presence of 3d cations in the infinite $(-M-U_3F_{22}-)_\infty$ pillars that couples the magnetic moment on the uranium atom with that of the magnetic transition metal cation. The pillars tend to align their magnetic moments in an antiparallel orientation, but their triangular lattice arrangement leads to frustration, resulting in a nonzero net moment for the magnetic unit cell. Achieving exchange coupling between U(IV) and

DOI: 10.1021/jacs.9b00345
J. Am. Chem. Soc. 2019, 141, 3838−3842

transition metal cations in triangular lattices is a highly promising outcome, as it identifies one structural requirements for future uranium(IV) magnetic materials.

■ ASSOCIATED CONTENT

Supporting Information

The Supporting Information is available free of charge on the ACS Publications website at DOI: 10.1021/jacs.9b00345.

Syntheses of the compounds, crystallographic data, EDS results, PXRD patterns, magnetic susceptibility plots, Rietveld refinement plots (PDF)
Crystallographic data for $Cs_2F_{16}U_3Zn$ (CIF)
Crystallographic data for $Cs_2F_{16}NiU_3$ (CIF)
Crystallographic data for $Cs_2F_{16}MnU_3$ (CIF)
Crystallographic data for $Cs_2F_{16}MgU_3$ (CIF)
Crystallographic data for $CoCs_2F_{16}U_3$ (CIF)

■ AUTHOR INFORMATION

Corresponding Author

*zurloye@mailbox.sc.edu

ORCID

Vladislav V. Klepov: 0000-0002-2039-2457
Hans-Conrad zur Loye: 0000-0001-7351-9098

Notes

The authors declare no competing financial interest.

■ ACKNOWLEDGMENTS

Research supported by the U.S. Department of Energy, Office of Basic Energy Sciences, Division of Materials Sciences and Engineering under award DE-SC0018739. This research used resources at the High Flux Isotope Reactor, a DOE Office of Science User Facility operated by the Oak Ridge National Laboratory.

■ REFERENCES

(1) *The Chemistry of the Actinide and Transactinide Elements*; Morss, L. R., Ed.; Springer: Dordrecht, 2010.
(2) MacDonald, M. R.; Fieser, M. E.; Bates, J. E.; Ziller, J. W.; Furche, F.; Evans, W. J. Identification of the + 2 Oxidation State for Uranium in a Crystalline Molecular Complex, [K(2.2.2-Cryptand)][$(C_5H_4SiMe_3)_3U$]. *J. Am. Chem. Soc.* **2013**, *135*, 13310−13313.
(3) Lussier, A. J.; Lopez, R. A. K.; Burns, P. C. A Revised and Expanded Structure Hierarchy of Natural and Synthetic Hexavalent Uranium Compounds. *Can. Mineral.* **2016**, *54*, 177−283.
(4) zur Loye, H.-C.; Besmann, T.; Amoroso, J.; Brinkman, K.; Grandjean, A.; Henager, C. H.; Hu, S.; Misture, S. T.; Phillpot, S. R.; Shustova, N. B.; et al. Hierarchical Materials as Tailored Nuclear Waste Forms: A Perspective. *Chem. Mater.* **2018**, *30*, 4475−4488.
(5) Wang, Y.; Yin, X.; Liu, W.; Xie, J.; Chen, J.; Silver, M. A.; Sheng, D.; Chen, L.; Diwu, J.; Liu, N.; et al. Emergence of Uranium as a Distinct Metal Center for Building Intrinsic X-Ray Scintillators. *Angew. Chem., Int. Ed.* **2018**, *57*, 7883−7887.
(6) Liu, W.; Dai, X.; Xie, J.; Silver, M. A.; Zhang, D.; Wang, Y.; Cai, Y.; Diwu, J.; Wang, J.; Zhou, R.; et al. Highly Sensitive Detection of UV Radiation Using a Uranium Coordination Polymer. *ACS Appl. Mater. Interfaces* **2018**, *10*, 4844−4850.
(7) Xie, J.; Wang, Y.; Silver, M. A.; Liu, W.; Duan, T.; Yin, X.; Chen, L.; Diwu, J.; Chai, Z.; Wang, S. Tunable 4f/5f Bimodal Emission in Europium-Incorporated Uranyl Coordination Polymers. *Inorg. Chem.* **2018**, *57*, 575−582.
(8) Gao, Y.; Szymanowski, J. E. S.; Sun, X.; Burns, P. C.; Liu, T. Thermal Responsive Ion Selectivity of Uranyl Peroxide Nanocages: An Inorganic Mimic of K^+ Ion Channels. *Angew. Chem., Int. Ed.* **2016**, *55*, 6887−6891.
(9) Payne, M. K.; Pyrch, M. M.; Jubinsky, M.; Basile, M. C.; Forbes, T. Z. Impacts of Oxo Interactions within Actinyl Metal Organic Materials: Highlight on Thermal Expansion Behaviour. *Chem. Commun.* **2018**, *54*, 10828−10831.
(10) Surbella, R. G.; Ducati, L. C.; Autschbach, J.; Deifel, N. P.; Cahill, C. L. Thermochromic Uranyl Isothiocyanates: Influencing Charge Transfer Bands with Supramolecular Structure. *Inorg. Chem.* **2018**, *57*, 2455−2471.
(11) Li, H.; Langer, E. M.; Kegler, P.; Modolo, G.; Alekseev, E. V. Formation of Open Framework Uranium Germanates: The Influence of Mixed Molten Flux and Charge Density Dependence in U-Silicate and U-Germanate Families. *Inorg. Chem.* **2018**, *57*, 11201−11216.
(12) Kindra, D. R.; Evans, W. J. Magnetic Susceptibility of Uranium Complexes. *Chem. Rev.* **2014**, *114*, 8865−8882.
(13) Kozimor, S. A.; Bartlett, B. M.; Rinehart, J. D.; Long, J. R. Magnetic Exchange Coupling in Chloride-Bridged 5f−3d Heterometallic Complexes Generated via Insertion into a Uranium(IV) Dimethylpyrazolate Dimer. *J. Am. Chem. Soc.* **2007**, *129*, 10672−10674.
(14) Chatelain, L.; Walsh, J. P. S.; Pécaut, J.; Tuna, F.; Mazzanti, M. Self-Assembly of a 3d-5f Trinuclear Single-Molecule Magnet from a Pentavalent Uranyl Complex. *Angew. Chem., Int. Ed.* **2014**, *53*, 13434−13438.
(15) Yeon, J.; Smith, M. D.; Tapp, J.; Möller, A.; zur Loye, H.-C. Application of a Mild Hydrothermal Approach Containing an in Situ Reduction Step to the Growth of Single Crystals of the Quaternary U(IV)-Containing Fluorides $Na_4MU_6F_{30}$ (M = Mn^{2+}, Co^{2+}, Ni^{2+}, Cu^{2+}, and Zn^{2+}) Crystal Growth, Structures, and Magnetic Properties. *J. Am. Chem. Soc.* **2014**, *136*, 3955−3963.
(16) Yeon, J.; Smith, M. D.; Morrison, G.; zur Loye, H.-C. Trivalent Cation-Controlled Phase Space of New U(IV) Fluorides, $Na_3MU_6F_{30}$ (M = Al^{3+}, Ga^{3+}, Ti^{3+}, V^{3+}, Cr^{3+}, Fe^{3+}): Mild Hydrothermal Synthesis Including an in Situ Reduction Step, Structures, Optical, and Magnetic Properties. *Inorg. Chem.* **2015**, *54*, 2058−2066.
(17) Le Borgne, T.; Rivière, E.; Marrot, J.; Thuéry, P.; Girerd, J.-J.; Ephritikhine, M. Syntheses, X-Ray Crystal Structures, and Magnetic Properties of Novel Linear MUIV Complexes (M = Co, Ni, Cu, Zn). *Chem. - Eur. J.* **2002**, *8*, 773−783.
(18) Mörtl, K. P.; Sutter, J.-P.; Golhen, S.; Ouahab, L.; Kahn, O. Structure and Magnetic Characteristics of an Oxalate-Bridged U(IV)−Mn(II) Three-Dimensional Network. *Inorg. Chem.* **2000**, *39*, 1626−1627.
(19) Chatelain, L.; Tuna, F.; Pécaut, J.; Mazzanti, M. A Zig-Zag Uranyl(v)−Mn(ii) Single Chain Magnet with a High Relaxation Barrier. *Chem. Commun.* **2015**, *51*, 11309−11312.
(20) Chemey, A. T.; Sperling, J. M.; Albrecht-Schmitt, T. E. Expanding Pentafluorouranates: Hydrothermal Synthesis and Characterization of β-$NaUF_5$ and β-$NaUF_5 \cdot H_2O$. *RSC Adv.* **2018**, *8*, 28642−28648.
(21) Chen, L.; Diwu, J.; Gui, D.; Wang, Y.; Weng, Z.; Chai, Z.; Albrecht-Schmitt, T. E.; Wang, S. Systematic Investigation of the *in Situ* Reduction Process from U(VI) to U(IV) in a Phosphonate System under Mild Solvothermal Conditions. *Inorg. Chem.* **2017**, *56*, 6952−6964.
(22) Lin, J.; Yue, Z.; Silver, M. A.; Qie, M.; Wang, X.; Liu, W.; Lin, X.; Bao, H.-L.; Zhang, L.-J.; Wang, S.; et al. In Situ Reduction from Uranyl Ion into a Tetravalent Uranium Trimer and Hexamer Featuring Ion-Exchange Properties and the Alexandrite Effect. *Inorg. Chem.* **2018**, *57*, 6753−6761.
(23) Xie, J.; Wang, Y.; Liu, W.; Yin, X.; Chen, L.; Zou, Y.; Diwu, J.; Chai, Z.; Albrecht-Schmitt, T. E.; Liu, G.; et al. Highly Sensitive Detection of Ionizing Radiations by a Photoluminescent Uranyl Organic Framework. *Angew. Chem., Int. Ed.* **2017**, *56*, 7500−7504.
(24) Yeon, J.; Smith, M. D.; Tapp, J.; Möller, A.; zur Loye, H.-C. Mild Hydrothermal Crystal Growth, Structure, and Magnetic Properties of Ternary U(IV) Containing Fluorides: $LiUF_5$, KU_2F_9, $K_7U_6F_{31}$, $RbUF_5$, RbU_2F_9, and RbU_3F_{13}. *Inorg. Chem.* **2014**, *53*, 6289−6298.

DOI: 10.1021/jacs.9b00345
J. Am. Chem. Soc. 2019, 141, 3838−3842

(25) Li, H.; Kegler, P.; Bosbach, D.; Alekseev, E. V. Hydrothermal Synthesis, Study, and Classification of Microporous Uranium Silicates and Germanates. *Inorg. Chem.* **2018**, *57*, 4745−4756.
(26) Klepov, V. V.; Felder, J. B.; zur Loye, H.-C. Synthetic Strategies for the Synthesis of Ternary Uranium(IV) and Thorium(IV) Fluorides. *Inorg. Chem.* **2018**, *57*, 5597−5606.
(27) Chen, L.; Zheng, T.; Bao, S.; Zhang, L.; Liu, H.-K.; Zheng, L.; Wang, J.; Wang, Y.; Diwu, J.; Chai, Z.; et al. A Mixed-Valent Uranium Phosphonate Framework Containing U^{IV}, U^{V}, and U^{VI}. *Chem. - Eur. J.* **2016**, *22* (34), 11954−11957.
(28) Felder, J. B.; Smith, M.; zur Loye, H.-C. $[Co(H_2O)_6]_3[U_2O_4F_7]_2$: A Model System for Understanding the Formation of Dimensionally Reduced Materials. *Cryst. Growth Des.* **2018**, *18*, 1236−1244.
(29) Jin, G. B.; Ringe, E.; Long, G. J.; Grandjean, F.; Sougrati, M. T.; Choi, E. S.; Wells, D. M.; Balasubramanian, M.; Ibers, J. A. Structural, Electronic, and Magnetic Properties of $UFeS_3$ and $UFeSe_3$. *Inorg. Chem.* **2010**, *49*, 10455−10467.
(30) Felder, J. B.; Calder, S.; zur Loye, H.-C. Retention of a Paramagnetic Ground State at Low Temperatures in a Family of Structurally Related U^{IV} Phosphates. *Inorg. Chem.* **2018**, *57*, 9286−9295.
(31) Felder, J. B.; Smith, M. D.; zur Loye, H.-C. Breaking a Paradigm: Observation of Magnetic Order in the Purple U(IV) Phosphite: $U(HPO_3)_2$. *Inorg. Chem.* **2018**, *57*, 9851−9858.
(32) Wedgewood, F. A.; Kuzneitz, M. Actinide Pnictides and Chalcogenides. I. Study of Magnetic Ordering and Ordered Moments in Uranium Monochalcogenides by Neutron Diffraction. *J. Phys. C: Solid State Phys.* **1972**, *5*, 3012−3020.
(33) van Doorn, C. F.; de V. du Plessis, P. Anomalies in the Elastic Constants of Antiferromagnetic Uranium Mononitride. *J. Magn. Magn. Mater.* **1977**, *5*, 164−166.
(34) Sidhu, S. S.; Vogelsang, W.; Anderson, K. D. The Antiferromagnetism of Uranium Monophosphide. *J. Phys. Chem. Solids* **1966**, *27*, 1197−1200.
(35) Calder, S.; An, K.; Boehler, R.; Dela Cruz, C. R.; Frontzek, M. D.; Guthrie, M.; Haberl, B.; Huq, A.; Kimber, S. A. J.; Liu, J.; et al. A Suite-Level Review of the Neutron Powder Diffraction Instruments at Oak Ridge National Laboratory. *Rev. Sci. Instrum.* **2018**, *89*, 092701.
(36) Garlea, V. O.; Chakoumakos, B. C.; Moore, S. A.; Taylor, G. B.; Chae, T.; Maples, R. G.; Riedel, R. A.; Lynn, G. W.; Selby, D. L. The High-Resolution Powder Diffractometer at the High Flux Isotope Reactor. *Appl. Phys. A: Mater. Sci. Process.* **2010**, *99*, 531−535.
(37) Perez-Mato, J. M.; Gallego, S. V.; Tasci, E. S.; Elcoro, L.; de la Flor, G.; Aroyo, M. I. Symmetry-Based Computational Tools for Magnetic Crystallography. *Annu. Rev. Mater. Res.* **2015**, *45*, 217−248.
(38) Greedan, J. E. Geometrically Frustrated Magnetic Materials. *J. Mater. Chem.* **2001**, *11*, 37−53.
(39) Bean, A. C.; Sullens, T. A.; Runde, W.; Albrecht-Schmitt, T. E. Hydrothermal Preparation of Nickel(II)/Uranium(IV) Fluorides with One-, Two-, and Three-Dimensional Topologies. *Inorg. Chem.* **2003**, *42*, 2628−2633.

DOI: 10.1021/jacs.9b00345
J. Am. Chem. Soc. 2019, 141, 3838−3842